

Advanced common control method for shunt and series active compensators used in power quality improvement

M.A.E. Alali, Y.-A. Chapuis, S. Saadate and F. Braun

Abstract: An advanced common control method for shunt and series active conditioners, which compensate for the main types of disturbances in electrical power systems, is considered. If shunt and series active conditioners are already well known as good compensation solutions for power quality improvement, it is also admitted that they generate some undesired components at switching frequency. To avoid these propagation problems, conditioner designers proposed a high-order output filter associated to a specific controller based on the RST control method. However, by applying this controller, it can be observed that a phase lag between the reference and the injected signal appears in the current and voltage control loop, which damages harmonic compensation. Therefore, a new RST controller is proposed, called RST_{imp} , to overcome the phase lag effects over the entire bandwidth for both active conditioners. The RST_{imp} proposed control method is validated through SABER simulations. These simulations show very good active conditioner performance in terms of rapidity, tracking and robustness for both current and voltage compensation.

1 Introduction

In most industrial countries, the shunt active conditioner is becoming an alternative solution to compensate for current disturbance in electrical installations [1]. However, shunt active conditioner inverters generate some undesired components at switching frequency. These components can be propagated through the output filter and affect line current and voltage. These effects can also appear with a PWM inverter with a high switching frequency. To avoid these effects, an auxiliary passive filter associated to a first-order output filter can be inserted either in the network side or at the inverter output. Unfortunately, this solution can cause secondary effects such as resonance problems. A solution is to include a third-order output filter, also called a T-type filter, with current control based on hysteresis or sliding mode [2]. However, this proposal causes switching frequency variation and consequently damages the power converter switches.

Finally, to overcome these problems, a PWM inverter with an RST controller for the current loop is proposed. In this case, the PWM inverter output voltage, and consequently the injected current of the shunt active conditioner, are controlled by the RST controller. However, this controller cannot guarantee good compensation. Although

the tracking of the magnitude of identified disturbances is quite good, phase lag between the reference and the injected signals appears in the current control loop.

For other disturbances such as voltage harmonics, unbalanced voltage and voltage sag, many studies have already addressed these problems. Series active conditioners compensate for unbalanced voltage and also voltage sag [3]. However, the phase lag effect, previously identified in the shunt active conditioner, prevents the series conditioner from compensating properly for voltage harmonics.

To solve all those problems, in both shunt and series active conditioners, this paper considers an improved common control method based on the RST controller, called RST_{imp} .

2 Active conditioner structures

2.1 General structure

The shunt active conditioner is generally composed of a control part and a power part, including a PWM voltage source inverter, a DC capacitive storage system and an output filter. In electrical power systems, most power quality problems are associated with voltage harmonics, unbalanced voltages and voltage sag. Voltage sags are generally caused by faults or starting currents of large power machines. However, unbalance and harmonic voltages are usually generated by unbalanced consumption and non-linear loads. They can also be caused by a disturbance or a distortion of the network EMF. Many series active conditioner structures have been proposed [4, 5]. One well-known structure includes a control part and a power part composed of a three-phase voltage PWM inverter, a DC capacitive storage system, an output filter and three single-phase transformers [6, 7].

In both active conditioner structures, the control part is composed of an identification method and a control loop of

© IEE, 2004

IEE Proceedings online no. 20040679

doi:10.1049/ip-epa:20040679

Paper first received 8th July 2003 and in revised form 30th April 2004. Originally published online: 14th September 2004

M.A.E. Alali is with the Faculty of Electrical Engineering, University of Aleppo, Aleppo, Syria

Y.-A. Chapuis and F. Braun are with the LEPSI-23, Rue du Loess, BP 20-67037 Strasbourg Cedex 2, France

S. Saadate is with the GREEN, France Université, Henri Poincaré, 54500 Vandoeuvre-lès-Nancy, France

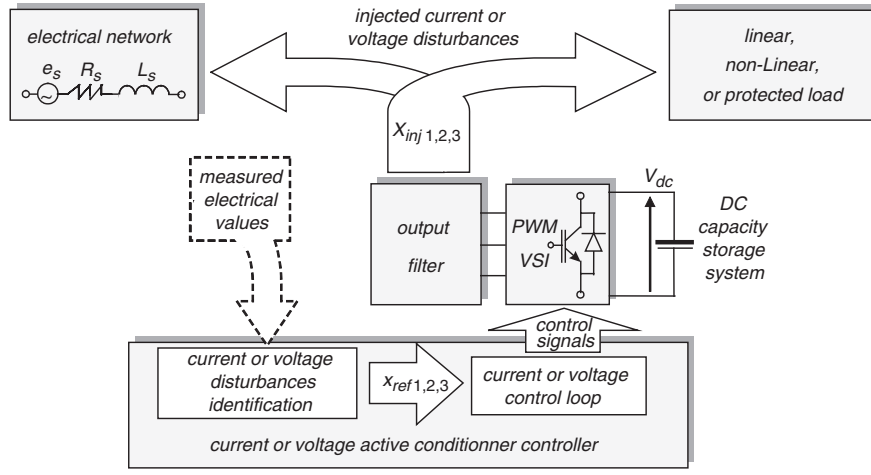


Fig. 1 Common structure of shunt and series active conditioners

the disturbance. We talk about identified current or voltage ($X_{ref1,2,3}$) and injected disturbance ($X_{inj1,2,3}$) for both shunt and series active conditioners. Figure 1 shows a common structure of shunt and series active conditioners and the power environment, including a three-wire power network and a non-linear or protected load.

2.2 Output current and voltage control

A three-phase voltage source inverter (VSI) is used to generate the current and voltage references that are injected to the network supply. The VSI is controlled by a PWM. The VSI is connected to the electrical network by a passive output filter. The output filter must be designed to reject components at the switching frequency generated by the PWM VSI.

2.2.1 Transfer functions of output filters: The output filter is modelled by the following equations:

$$X_{inj}(s) = \frac{B_1(s)}{A(s)} V_{inv}(s) + \frac{B_2(s)}{A(s)} X_{per}(s) \quad (1)$$

$$\text{with} \begin{cases} A(s) = a_1 s^n + a_2 s^{n-1} + \dots + a_n s + a_{n+1} \\ B_1(s) = b_{11} s^{n-2} + b_{12} s^{n-3} + \dots + b_{1(n-2)} s + b_{1(n-1)} \\ B_2(s) = b_{21} s^{n-1} + b_{22} s^{n-2} + \dots + b_{2(n-1)} s + b_{2n} \end{cases} \quad (2)$$

$B_1(s)/A(s)$ is the transfer function of the output filter and $B_2(s)/A(s)$ represents a disturbance model. $V_{inv}(s)$ is the inverter output voltage and $X_{per}(s)$ is considered as a disturbance. n is the order of the output filter transfer function.

2.2.2 Shunt active conditioner: third-order output filter: For a better filtering of the switching frequency, a T-type third-order output filter is proposed (cf. Table 1). The transfer functions of the output filter and

Table 1: Electrical network characteristics

	Shunt active conditioner	Series active conditioner
Electrical network (1 MVA, $u_{cc} = 4\%$)	$R_s = 0.25 \text{ m}\Omega$; $L_s = 19.4 \text{ }\mu\text{H}$	
Output Filter	<p>1st Order Filter</p> <p>$L_f = L_{f1} + L_{f2}$ $R_f = R_{f1} + R_{f2}$</p>	
	<p>T-type Filter (3rd Order Filter)</p> <p>$L_{f1} = 90 \text{ }\mu\text{H}$, $R_{f1} = 5 \text{ m}\Omega$; $L_{f2} = 70 \text{ }\mu\text{H}$, $R_{f2} = 5 \text{ m}\Omega$; $L_f = 200 \text{ }\mu\text{H}$, $R_f = 160 \text{ m}\Omega$;</p>	
	<p>2nd Order Filter</p> <p>$R_{sf} = 25 \text{ m}\Omega$; $L_{sf} = 400 \text{ }\mu\text{H}$; $C_{sf} = 250 \text{ }\mu\text{F}$</p>	
Storage capacitor	$C_d = 4.4 \text{ mF}$; $V_{dc} = 840 \text{ V}$	Direct source: $V_{dc} = 840 \text{ V}$
Cut-off frequency of the output filter	1900 Hz	500 Hz
Switching frequency	12.5 KHz	12.5 KHz

disturbance model are given by:

$$\begin{cases} a_1 = (L_s + L_{f2})L_{f1}C_f \\ a_2 = \left[(L_s + L_{f2})R_{f1}C_f + (R_s + R_{f2})L_{f1}C_f + \right. \\ \quad \left. + (L_{f1} + L_s + L_{f2})R_fC_f \right] \\ a_3 = \left[(L_s + L_{f2}) + L_{f1} + (R_s + R_{f2})R_{f1}C_f + \right. \\ \quad \left. + (R_{f1} + R_s + R_{f2})R_fC_f \right] \\ a_4 = R_{f1} + R_s + R_{f2} \end{cases}$$

$$\text{and } \begin{cases} b_{11} = R_f C_f \\ b_{12} = 1 \\ b_{21} = L_f C_f \\ b_{22} = (R_f + R_{f1}) \\ b_{23} = 1 \end{cases} \quad (3)$$

2.2.3 Series active conditioner: second-order output filter: The series active conditioner structure uses a passive output filter (L_{sf} , R_{sf} , C_{sf}) of second order (cf. Fig. 1 and Table 1). The transfer functions can be obtained from the following parameters:

$$\begin{cases} a_1 = L_{sf} C_{sf} \\ a_2 = L_{sf} C_{sf} \\ a_3 = 1 \end{cases} \quad \text{and} \quad \begin{cases} b_{11} = 1 \\ b_{21} = L_{sf} \\ b_{22} = R_{sf} \end{cases} \quad (4)$$

3 Control methods

The cut-off frequency of the closed-loop control must be high enough not to modify the reference signal (X_{ref}). This frequency must also be far enough from the switching frequency to model the inverter as a simple gain. The control criteria of the closed loop must ensure good reference tracking and short response time. We propose in a first approach to study an RST control method.

3.1 RST control method

3.1.1 Common control method principle: The RST controller is based on a pole-placement design, as shown in the general scheme of Fig. 2. This method can satisfy most control criteria such as good robustness. For the shunt active conditioner, the disturbances (X_{per}) are caused by the network voltage $V_s(s)$. In this paper, the effect of this type of disturbance is compensated for by adding the same network voltage to the control signal $u(s)$, as shown in Fig. 2. This voltage is necessary to prevent the fundamental current from passing from the network to the active conditioner.

For the series active conditioner, the disturbances (X_{per}) are caused by the load current (I_L). Indeed, the load current crosses the active conditioner and disturbs the injection voltage (V_{inj}). In this paper, this type of disturbance is

compensated for by the closed loop, as shown later. From Fig. 2 and (1), we can write the following equation:

$$X_{inj}(s) = \frac{(TB_1)(s)}{(SA + B_1R)(s)} X_{ref}(s) + \frac{(SB_2)(s)}{(SA + B_1R)(s)} X_{per}(s) \quad (5)$$

where $R(s)$, $S(s)$ and $T(s)$ are the controller polynomials. The two parts of (5) represent the closed-loop transfer function in terms of tracking and disturbance effects. The order of $R(s)$ and $S(s)$ is the same as the output filter $B_1(s)/A(s)$. Thus, from (3) and (4), the order of $R(s)$ and $S(s)$ is $n=3$ for the current control loop and $n=2$ for the voltage control loop. $T(s)$ can be given by a simple gain as $X_{inj}(s)/X_{ref}(s)=1$ when the Laplace variable (s) tends to 0.

3.1.2 Phase lag effect problems: The RST control method is generally used when the reference to be tracked is either a constant or a single-frequency signal with relatively low frequency. In the single-frequency case, phase lag (γ) between reference (X_{ref}) and injected (X_{inj}) signals is acceptable. However, the phase lag is unacceptable when the reference signal includes multiple frequencies, as phase lag increases with frequency. Moreover, the higher the order of the controlled system, the higher the phase lag is. Figure 3 illustrates the phase lag effect for a distorted signal (X_{sig}), which is not correctly compensated for (X_{real}), compared to the ideal form (X_{ideal}).

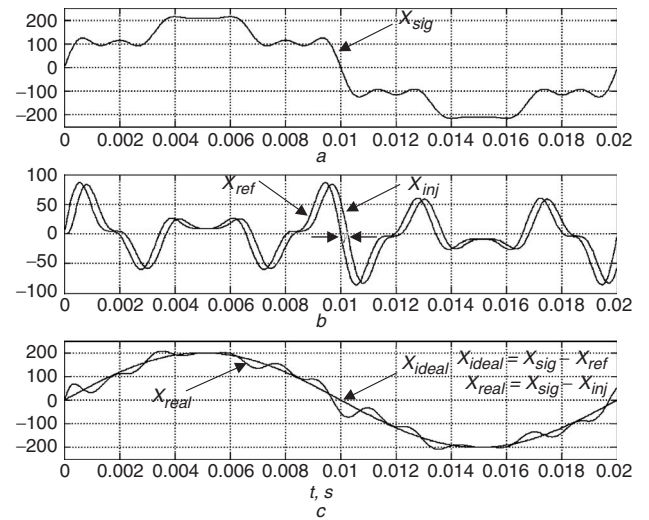


Fig. 3 Phase lag effect on compensation quality

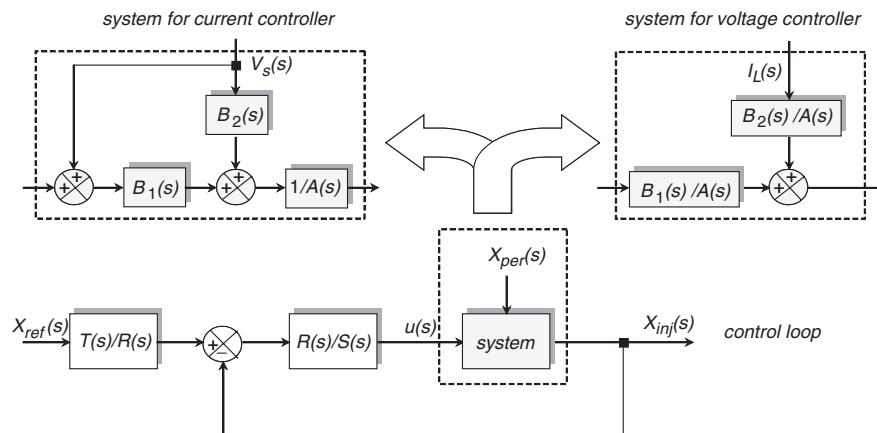


Fig. 2 General RST controller scheme

3.2 Improved RST control method (RST_{imp})

To overcome the phase lag effect and achieve good compensation performance, a first approach was to propose linear controllers, such as PI, PID, H_2 , H_∞ etc. However, as they were initially proposed in the literature, these solutions amplified more than they reduced the phase lag problem.

Recently, new robust controllers based on H_2 and H_∞ modes have been proposed in the literature to compensate for these undesired effects [8, 9]. In this context, we propose a control method based on an advanced linear control mode, which treats particularly the phase lag problem. This advanced control method is based on the same principle used in a classic RST where zeros have been placed in the transfer function of the closed loop. These zeros are placed to reduce gain and phase error. Error minimisation $e(s)$ is determined by the equation from Fig. 2:

$$e(s) = (X_{inj} - X_{ref})(s) = \left(\frac{(TB_1)(s)}{D(s)} - 1 \right) X_{ref}(s) \quad (6)$$

whose $D(s) = (AS + B_1R)(s)$ (arbitrary stability polynomial).

From (6), we can obtain the transfer function as given by:

$$\frac{e(s)}{X_{ref}(s)} = \left(\frac{(TB_1 - D)(s)}{D(s)} \right) \quad (7)$$

To reduce the error $e(s)$ to zero, the numerator of (7) must tend to zero. Since $R(s)$ and $S(s)$ are already defined, only $T(s)$ can reduce the error $e(s)$. Moreover, the order of $T(s)$ must be chosen so that the transfer function $T(s)/R(s)$ (cf. Fig. 2) is causal (degree(T) ≤ degree(R)), as given in (8). The stability of the system, defined by a classic RST method, is not modified if the $T(s)$ polynomial is stable:

$$T(s) = t_1s^n + t_2s^{n-1} + \dots + t_ns + t_{n-1} \quad (8)$$

By using (8) and replacing $s = j\omega$ with ω the angular frequency, the numerator of (7) becomes:

$$(TB_1 - D)(j\omega) = R_e(\omega) + jI_m(\omega) \quad (9)$$

To make (9) tend to zero, both the real $R_e(\omega)$ and imaginary $I_m(\omega)$ parts must tend to zero. This constraint means that there are two equations for each frequency of a placed zero. In this study, $T(s)$ is a third-order and second-order polynomial for current and voltage control, respectively.

For current control, a third-order $T(s)$ polynomial is the maximum order satisfying the causality of the transfer function $T(s)/R(s)$. Taking account of the unknown parameters in this case (t_1, t_2, t_3, t_4), only two frequencies have to be chosen. Zeros should be placed near the slowest poles of the closed-loop transfer function.

For the voltage control case, $T(s)$ is a second-order polynomial, which is the maximum order that still respects the causality of $T(s)/R(s)$ transfer function (cf. Fig. 2). Taking account of the unknown parameters in this case (t_1, t_2, t_3), two frequencies have to be chosen. Zeros are again placed near the slowest poles of the closed-loop transfer function.

3.3 Control method synthesis

3.3.1 Current control loop: Figure 4 and Table 2 compare current reference tracking of the RST and RST_{imp} control methods. Gain and phase of the transfer function of the current closed loop $I_{inj}(s)/I_{ref}(s)$ are given in Table 2 for multiples of the fundamental frequency (F_f), from F_f to $31 F_f$. In both control methods, gain remains at 0 dB for all frequencies, as shown in the Table 2.

The RST control method is only used to compensate for unbalanced current or reactive current which occurs at the fundamental frequency 50 Hz. At this frequency, a phase lag of (-1.116°) is negligible. Beyond this, phase lag is no longer negligible and the shunt active conditioner cannot compensate for current harmonics. The improved RST control method works for phase lag over the entire bandwidth. In this method, little overshoot occurred at the cut-off frequency of the closed loop, as shown in Fig. 4a. This frequency is high enough so that there is no risk of having a harmonic current component. Furthermore, a little dip between 650 and 1150 Hz can be observed in Fig. 4b. This dip is caused by the order of the $T(s)$ polynomial, which is 3 in this study and insufficient to ensure zero phase lag. Indeed, the polynomial degree of $T(s)$ is limited by the causality of the transfer function $T(s)/R(s)$ (cf. Fig. 2).

3.3.2 Voltage control loop case: Figure 5 and Table 3 compare the signal reference tracking of the two control methods. In Table 3, gain and phase of the transfer function $V_{inj}(s)/V_{ref}(s)$ of the closed loop are given for each method (RST, RST_{imp}). For all frequencies, gains are satisfactory with the two methods, as shown in Table 3.

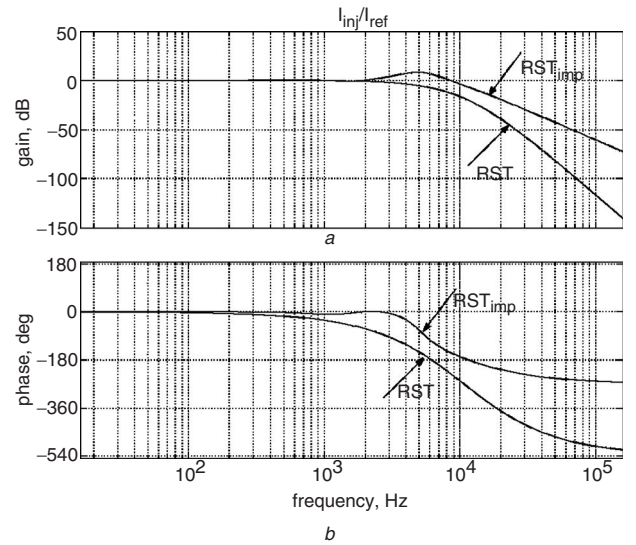


Fig. 4 Closed-loop transfer function with RST and RST_{imp} controllers

Table 2: Two control methods comparison for current control (RST and RST_{imp})

$F, \text{ Hz}$		50	250	350	550	650	850	950	1150	1250	1450	1550
RST	Gain, dB	1	1	1	1	0.99	0.98	0.98	0.97	0.97	0.95	0.94
	Phase, deg	-1	-8	-11	-18	-21	-27	-30	-37	-40	-46	-49
	Gain, dB	1	1	1	1.1	1.1	1	0.98	0.9	0.9	0.9	0.9
RST_{imp}	Phase, deg	-0.01	-0.54	-1.35	-4.36	-6.4	-10.1	-11.2	-10.2	-9.78	-6.50	-4.78

The RST method is only used to compensate for voltage sag or unbalance voltage which occurs at 50 Hz. At this frequency, the resulting phase lag (-1.278°) can be considered negligible. Above this frequency, phase lag is no longer negligible and the series active conditioner cannot compensate for voltage harmonics. The improved RST control method is valid for all bandwidth frequencies. Noted that a little overshoot occurs at the cut-off frequency where there is no risk of having a voltage harmonic component.

4 Simulation results

4.1 Shunt active conditioner application

The network is made up of a sub-transformer 20/0.4 kV, 1 MVA, $u_{cc} = 4\%$. The non-linear load is a 100 kVA six-pulse thyristor rectifier. A 100 kW linear unbalanced load is connected in parallel with the non-linear load. The shunt active conditioner is tested in two simulation cases. In these simulations, the shunt active conditioner has a T-type output filter and injected current is controlled by the RST_{imp} controller. Direct voltage storage capacitor V_{dc} is regulated by a PI controller. The shunt active conditioner recharges the capacitor.

The system rating values considered in the general structure are given in Table 1.

4.1.1 Current harmonic compensation: In the first simulation case, current harmonics generated by the non-linear load with a triggering angle $\alpha = 0^\circ$ was applied. Figure 6 shows the results, for phase 1, of nonlinear load current (I_{N-L1}), the superposition of current reference and injected current (I_{ref1} , I_{inj1}) and source line current (I_{L1}).

From Fig. 6, we remark that there is no phase lag between current reference and injected current. Thus, the

source line current pattern is good. The phase 1 current THD was been 21.16% for the nonlinear load and 1.5% for the source current after compensation.

To show the efficiency of the T-type output filter in switching frequency filtering, another simulation in almost the same conditions is illustrated in Fig. 7. The T-type output filter is replaced by a first-order filter which consists of one reactance with its inner resistor, as given in Table 1.

As can be observed in Fig. 7, the switching frequency components included in the injected current (I_{inj1}) prevent us from estimating the good tracking of the identified harmonics (I_{ref1}). The spectrum analysis has shown that for conventional harmonics, we have almost the same THD as with the T-type filter. On the other hand, taking account of the switching frequency, the THD of non-linear load current becomes 13.9%. This result demonstrates clearly the pertinence of using a high-order output filter.

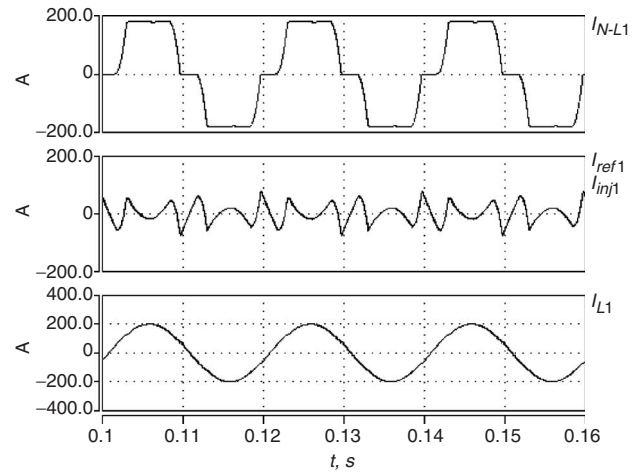


Fig. 6 Transient analysis of current harmonic compensation

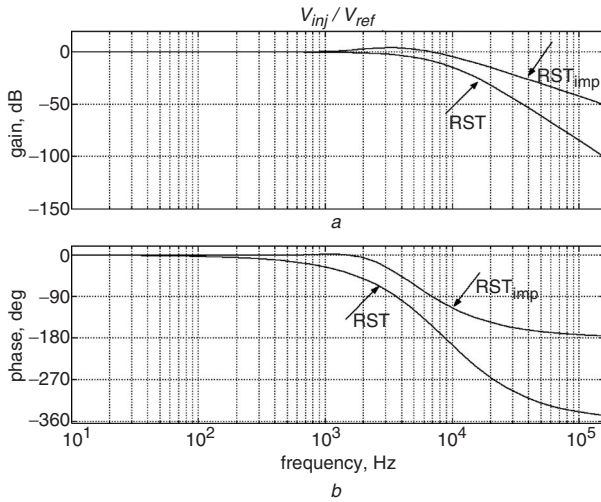


Fig. 5 Closed-loop transfer function with RST and RST_{imp} controllers

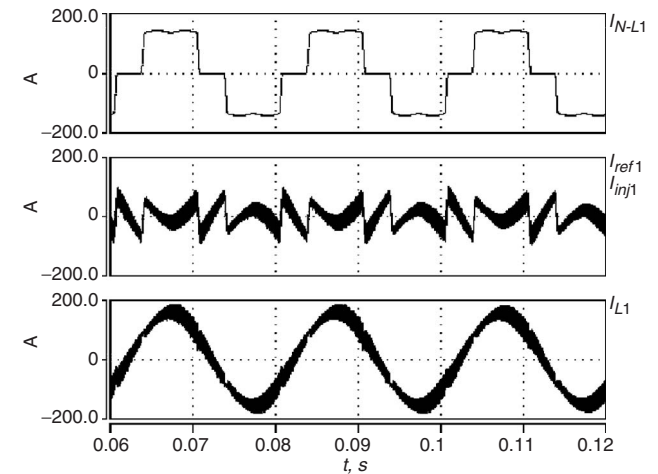


Fig. 7 Switching frequency effect on harmonics compensation

Table 3: Two control methods comparison for voltage control (RST and RST_{imp})

F , Hz		50	250	350	550	650	850	950	1150	1250
RST	Gain, dB	1	1	1	1	1	1.05	1.05	1.1	1.1
	Phase, deg	-1	-6	-9	-14	-17	-22	-24	-29	-32
RST_{imp}	Gain, dB	1	1	1	1	1	1.06	1.07	1.2	1.24
	Phase, deg	-0.15	-0.5	-0.5	0.3	0.7	1.5	1.5	0.5	-0.8

4.1.2 Current harmonic, reactive power and negative sequence current compensation:

In this simulation, shunt active conditioner was studied to compensate for current harmonics, reactive power and negative sequence current caused by an unbalanced linear load. Reactive power is caused by the triggering angle $\alpha = 42^\circ$. Figure 8 shows simulation results of transient analysis for this case. The three-phase non-linear load current ($I_{N-L1,2,3}$), unbalanced linear load current ($I_{L-L1,2,3}$) and source current ($I_{L1,2,3}$) are presented. Current reference and injected current ($I_{ref1,2,3}$, $I_{inj1,2,3}$) are superimposed for each phase. There is no phase lag between current reference and injected current. Current source patterns prove that the compensation quality is good. Indeed, the current source is balanced and almost harmonic free. The source current

phase angle is zero, which demonstrates good power factor compensation.

4.2 Series active conditioner application

The supply is from a sub-transformer 20/0.4 kV, 1 MVA, $u_{cc} = 4\%$. The load is a 100 kVA series $R-L$, with a peak current of $\hat{I} = 205$ A, and power factor $\cos \varphi = 0.8$. The system rating values are given in Table 1.

4.2.1 Single-phase voltage sag compensation:

Figure 9 shows a transient analysis using an RST controller for an 80% single-phase voltage sag on phase 1. From these results, a negative voltage rate of 36% is obtained for the network side, compared to 0.669% for the load side after compensation. Moreover, since reference

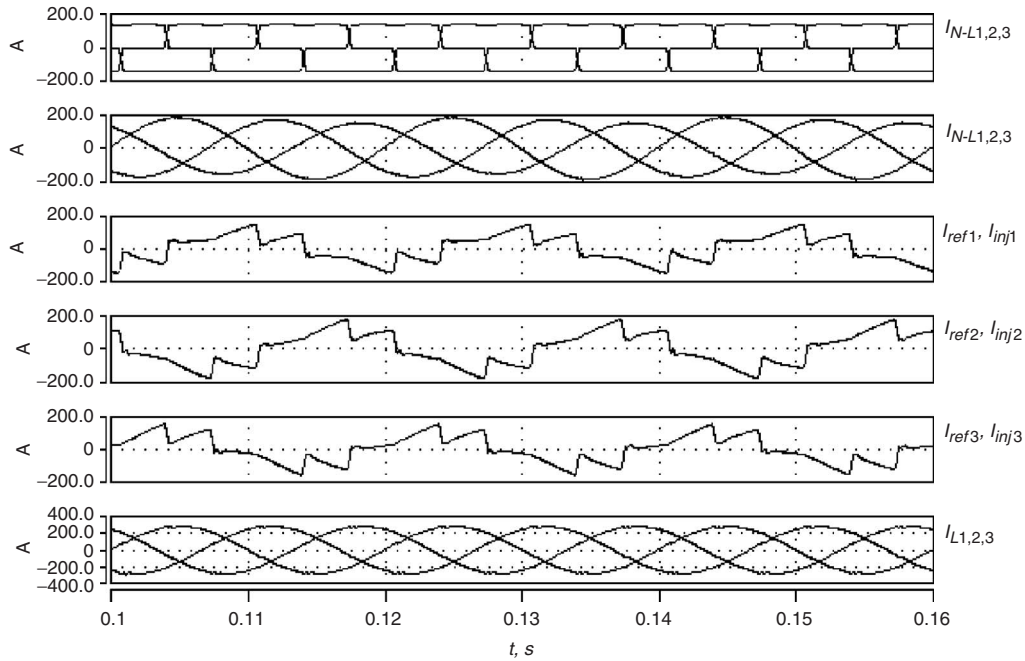


Fig. 8 Transient analysis of current disturbances compensation

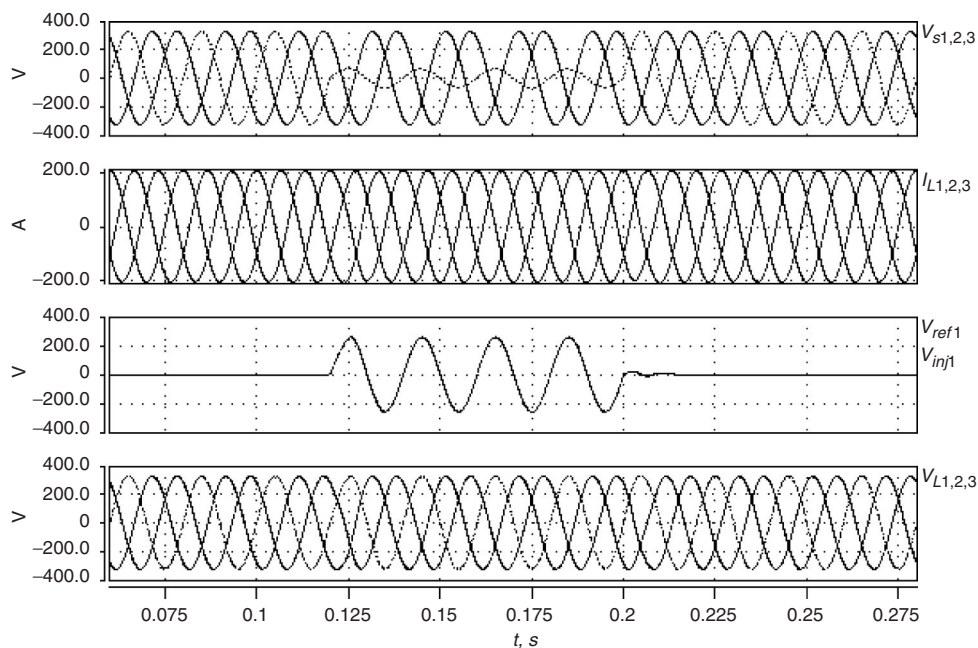


Fig. 9 Transient analysis of voltage sag compensation using RST

tracking time is negligible, compensation can be considered instantaneous.

The simulation results for the same case using the RST_{imp} controller are very satisfactory [7]. Indeed, the load voltage amplitude is 324.2 and 324.95 V by using RST and RST_{imp} , respectively. The gain and phase at fundamental frequency, given in Table 3, explain these results which, in addition to the almost instantaneous response, show the effectiveness of the two controllers for this type of disturbance.

4.2.2 Unbalance voltage and voltage harmonics compensation: For this case, an unbalanced voltage and voltage harmonics compensation was studied. The three phase voltages $V_{s-max1} = 216$ V, $V_{s-max2} = 263$ V, $V_{s-max3} = 295$ V having, respectively, the phases 15° , -130° , 110° , cause a negative voltage rate of 13.6%. Voltage harmonic compensation concerns only the 5th, 7th, 11th and 13th harmonics with individual harmonic distortion rates of 10, 7, 1 and 1%, respectively, compared to the nominal voltage of 325 V. Only one control method is proposed in this part: the RST_{imp} controller. Indeed, the RST controller, handicapped by the phase lag as given in Table 3, could not guarantee good compensation.

Transient analysis is illustrated in Fig. 10 After compensation, negative voltage ratio is 0.015% for the load side. The angle of voltage load becomes 3.2° for phase 1, shifted by -120° and $+120^\circ$ for phases 2 and 3, respectively.

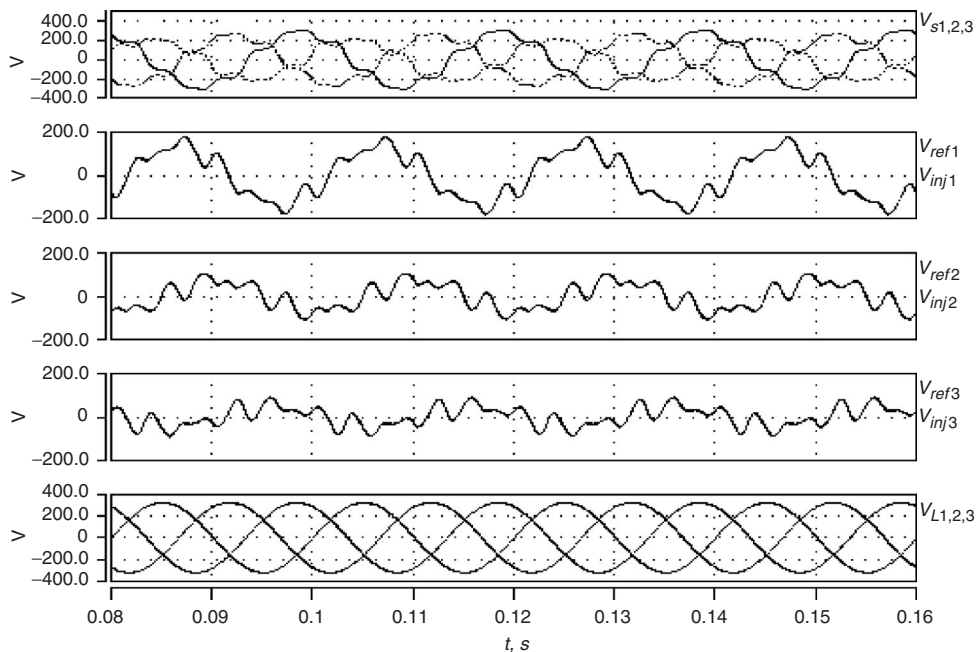


Fig. 10 Voltage sag and voltage harmonic compensation using RST_{imp}

The simulations prove that the proposed designs meet the objective of good tracking and consequently realise a good compensation of all electrical disturbances. These designs present a neutral function under perfect conditions of the electrical network. Indeed, when there is no voltage sag on phase 1, the identified and the injected signals are almost zero. If the proposed equipment does not achieve the required perfect performance (tracking), this is due to the non-zero phase lags, even at 50 Hz. In addition to the PLL (phase-locked loop) effect which, if it can guarantee an accurate delivery of the positive sequence voltage angle and magnitude, its precision cannot be naturally perfect [7, 10].

5 Conclusion and discussion

In this paper, shunt and series active conditioners using an advanced common control method have been studied in order to improve power quality in electrical network. This study is based on a third- and a second-order output filter proposed, respectively, for the shunt and series active conditioners, to ensure that the switching frequency has been filtered out of the injected signal. However, such compensation conditions require a specific controller, such as the improved control method called RST_{imp} , proposed in this paper. The RST_{imp} controller allows good performances in terms of rapidity, tracking and robustness to compensate for both current and voltage disturbances at the fundamental and harmonic frequencies, while overcoming phase lag that can appear in classic RST controllers.

The good results in compensation obtained by the proposed specific control method, RST_{imp} , promise a future trend for modern control methods such as robust control, optimal control, adaptive control etc. The controllers based on these methods have to take into consideration the new problems of magnitude and phase tracking, over a large frequency band. The tracking has to be performed almost perfectly with a good robustness and a short response time, without increasing the controller's order to assure its hardware realisation. These constraints are a good challenge

to the designers who work in the electrical, automation and microelectronics fields.

The choice of a relatively high switching frequency is in fact an advantage for the proposed control methods, without compromising a practical realisation. Indeed, for the active filters intended to compensate for current harmonics generated by a 100 kVA non linear load, a 12.5 kHz switching frequency is largely applicable for the new generation of IGBTs, noting that the power rating of the active filter in this case is almost 30 kVA [6]. For larger loads, we consider that a parallel connection of the active filters with the same switching frequency can be realised.

All our research work covered by this paper, modelling, design and simulation, has been made in continuous time mode. For an eventual hardware discrete time realisation, all the models and designs have to be made directly in discrete time. Then, the controller has new constraints such as Nyquist frequency, sampling frequency, sampling time etc. These new aspects need more space to be discussed.

6 References

- 1 Akagi, H.: 'New trends in active filters for power conditioning', *IEEE Trans. Ind. Appl.*, 1996, **32**, (6), pp. 1312–1322
- 2 Lapena, O.L., de Vicuna, L.G., Matas, J., Lopez, M., and Castilla, M.: 'A sliding mode control design of an active power filter with a low-pass filter as input stage'. Presented at EPE-99, Lausanne, Switzerland, 1999 (CD-ROM)
- 3 Sannino, A., and Svensson, J.: 'A series connected voltage source converter for voltage sag mitigation using vector control and a filter compensation algorithm'. Presented at the 35th IAS annual meeting of the 2000 IEEE Industry Applications Conf., Roma, Italy, October 2000, pp. 2476–2481
- 4 Visoser, A.J., Mouton, T., and Enslin, J.H.R.: 'Directed-coupled cascaded multilevel sag compensator'. Presented at the 31st IEEE annual Power Electronics Specialists Conference (PESC), Galway, Ireland, 2000 (CD-ROM)
- 5 Alarcon, G., Nunez, C., Cardenas, V., and Olivier, M.: 'Design and implementation of a 3-phase series active filter to compensate voltage disturbance'. Presented at CIEP-2000, Acapulco, Mexico, October 2000, pp. 93–98
- 6 Alali, M.A.E., Saadate, S., Chapuis, Y.A., and Braun, F.: 'Energetic study of a series active conditioner compensating voltage dips, unbalanced voltage and voltage harmonics'. Presented at CIEP-2000, Acapulco, Mexico, October 2000, pp. 80–86
- 7 Alali, M.A.E., Chapuis, Y.A., Braun, F., Zhou, L., and Saadate, S.: 'Advanced corrector with FPGA-based PLL to improve performance of series active filter compensating all voltage disturbances'. Presented at EPE-2001, August 2001, Graz, Austria (CD-ROM)
- 8 Ledwich, G., and Ghosh, A.: 'A flexible DSTATCOM operating on voltage or current control mode', *IEE Proc., Genes. Transm. Distrib.*, 2002, **149**, (2), pp. 215–224
- 9 Ledwich, G., and Ghosh, A.: 'Compensation of distribution system voltage using DVR', *IEEE Trans. Power Deliv.*, 2002, **17**, (4), pp. 1030–1036
- 10 Kaura, V., and Blasko, V.: 'Operation of a phase locked loop system under distorted utility conditions', *IEEE Trans. Ind. Appl.*, 1997, **33**, (1), pp. 58–63